JOURNAL OF SOLID STATE CHEMISTRY 107, 387–396 (1993)

The New Series of Fluoride Perovskites $Na_4Ba_xM_{4-x}F_{12}$ (M = Mn, Fe, Co) and $Na_{4-x}Li_xBa_xCo_{4-x}F_{12}$: Homogeneity Range and Crystal and Magnetic Structures

M. DUCAU, T. ROISNEL,* AND J. DARRIET

*Laboratoire de Chimie du Solide du CNRS, Université de Bordeaux I, 351 Cours de la Libération, 33405 Talence Cedex, France; and *Laboratoire Léon Brillouin (CEA-CNRS), Centre d'Etudes de Saclay, 91191 Gif sur Yvette Cedex, France*

Received January 28, 1993; in revised form March 31, 1993; accepted April 1, 1993

Investigation of the ternary systems containing AF–BaF_2–MF_2 (A = Li, Na; M = Mn, Fe, Co) shows the existence of a new series of perovskite-type structures $Na_4Ba_xM_{4-x}F_{12}$ (M = Mn, Fe, Co) and $Na_{4-x}Li_xBa_xCo_{4-x}F_{12}$, isostructural to $Na_4Ba_xFe_{4-x}F_{12}$ (x = 0.84), the structure of which has been determined from X-ray single-crystal data. In each system, the homogeneity range of the phases has been determined. The space group is $Im3$ with a unit-cell constant which is twice that of the parent ABX_3 perovskite. The cationic distribution in the different sites can be expressed by the detailed formula $[Ba_xNa_{1-x}]Na_3(Fe_{4-x}Na_x)F_{12}$ (x = 0.84). A Rietveld profile analysis from X-ray spectra for the cobalt phases and from neutron diffraction spectra for the manganese and iron phases confirmed the same cationic distribution. The magnetic properties of these fluorides, at low temperature, are characteristic of a 3D antiferromagnetic order. The magnetic structures of $Na_4Ba_xMn_{4-x}F_{12}$ (x = 0.75) and $Na_4Ba_xFe_{4-x}F_{12}$ (x = 0.87) have been determined.

Introduction

The studies of ternary systems containing barium fluoride, alkaline fluorides, and divalent fluorides of transition elements have shown that the number of quaternary phases is very limited. For instance, in the system NaF–BaF_2–CuF_2, only one phase of formula $Na_4BaCu_3F_{12}$ has been isolated (*1, 2*). The framework corresponds to a distorted superstructure of the perovskite with the copper ions and one-fourth of the sodium ions occupying the octahedral sites. In the system CsF–BaF_2–CuF_2, the compound $Cs_2Ba_2Cu_3F_{12}$ has been isolated, the structure of which is also characterized as a tetragonal perovskite with ordered octahedral vacancies (*3*). Our recent investigation of the ternary systems NaF–BaF_2–FeF_2 evidenced the existence of a new cubic phase $Na_4Ba_xFe_{4-x}F_{12}$ (x = 0.84) (*4*). Its structure has been determined by single-crystal X-ray diffraction. The framework has a perovskite-like arrangement in which the tilting of the BX_6 octahedra around one of their three axes creates two distinct sites: the A-sites (CN = 12) as in the ABX_3-perovskite structure are occupied by Ba and Na in the atomic ratio r = Na/Ba = $1 - x/x$, and the C-sites corresponding to a triangular prism (CN = 6) are occupied by the Na atoms. These atoms are localized in a 12e position with an occupied rate of 50%. In fact they are displaced off a planar environment (CN = 4). The structure is closely related to a series of homologous oxides $[AC_3]B_4O_{12}$, where the C-sites are occupied by Jahn-Teller cations such as Cu^{2+} or Mn^{3+} (this is the reason why the environment is planar) (*5–8*). The other difference is that the octahedral site, in the fluoride compound, is occupied by Fe and Na with a ratio $r = 4 - x/x$ (Fig. 1). The formula, on taking into account the cationic repartitions, becomes $[Ba_xNa_{1-x}]Na_3(Fe_{4-x}Na_x)F_{12}$ (x = 0.84). It appears that the structure is highly

0022-4596/93 $5.00

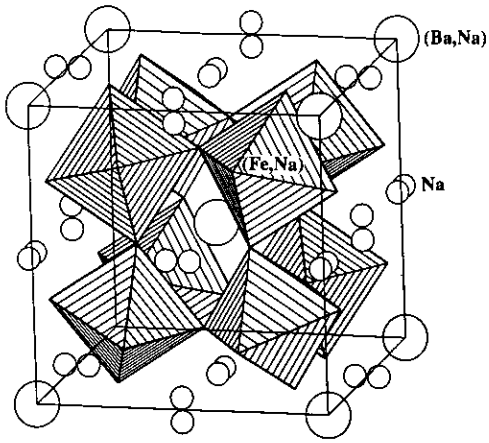

FIG. 1. The cubic crystal structure of $Na_4Ba_xFe_{4-x}F_{12}$ ($x = 0.84$).

disordered and a homogeneity range of this phase can be anticipated.

This paper reports the determination of the domains of stability and the structural studies of isostructural compounds corresponding to the substitution of Fe by Mn or Co as well as the substitution of Na by Li in the octahedral sites in the case of the cobalt phase.

Experimental

Syntheses

The compounds $Na_4Ba_xM_{4-x}F_{12}$ (M = Mn, Fe, Co) have been synthesized from stoichiometric mixtures of the corresponding binary fluorides with a heat treatment at 700°C for 1 day followed by annealing at 600°C for 2 days. The solid-state reactions have been carried out in platinum tubes sealed under dry argon atmosphere. With the same experimental conditions, the selective substitution of Na by Li has been possible only in the case of the cobalt phase.

Magnetic Measurements

The magnetic susceptibilities have been determined using a SQUID magnetometer (SHE Corp.) in the temperature range $6\ K < T < 250\ K$ with a magnetic field of 10 kG.

Neutron Diffraction

The experiments were performed on a G41 two-axes spectrometer, located in the neutron guide hall of the Orphée Reactor (Saclay). Data were recorded at different temperatures ($1.6\ K < T < 60.8\ K$) with a neutron wavelength of 2.426 Å. The 7°–87° angular 2Θ range has been explored (800-cell BF_3 multidetector). Using data below T_N, the nuclear and magnetic structures of $Na_4Ba_xMn_{4-x}F_{12}$ ($x = 0.75$) and $Na_4Ba_xFe_{4-x}F_{12}$ ($x = 0.87$) have been refined by a Rietveld profile analysis (*9*, *10*) from powder preparation samples of "$Na_4BaM_3F_{12}$" (M = Mn, Fe) which correspond to a mixture of the cubic phase and small quantities of NaF and BaF_2. Neutron scattering lengths have been taken as $b_{Ba} = 0.528 \times 10^{-12}$ cm, $b_{Na} = 0.363 \times 10^{-12}$ cm, $b_{Fe} = 0.954 \times 10^{-12}$ cm, $b_{Mn} = -0.373 \times 10^{-12}$ cm, and $b_F = 0.566 \times 10^{-12}$ cm; the Fe^{2+} and Mn^{2+} magnetic form factor was extracted with the calculation of Lisher and Forsyth (*11*).

Results and Discussion

Homogeneity Range

The phases $[Ba_xNa_{1-x}]Na_3(M_{4-x}Na_x)F_{12}$ (M = Mn, Fe, Co) belong to the pseudobinary systems $NaMF_3$–"$BaNaF_3$," where $BaNaF_3$ corresponds to the mixture of BaF_2 and NaF, as well as $[Ba_xNa_{1-x}]Na_3(Co_{4-x}Li_x)F_{12}$ belongs to the system $NaCoF_3$–$BaLiF_3$. By preparing several compositions in those systems, a domain of stability for each system has been observed, the limits of which are given in Table I.

TABLE I

LIMITS OF THE DOMAINS OF STABILITY OF THE PHASES $Na_4Ba_xM_{4-x}F_{12}$

M	x
Mn	$0.73 < x < 0.75$
Fe	$0.80 < x < 0.87$
Co	$0.85 < x < 0.93$
Co–Li	$0.62 < x < 0.69$

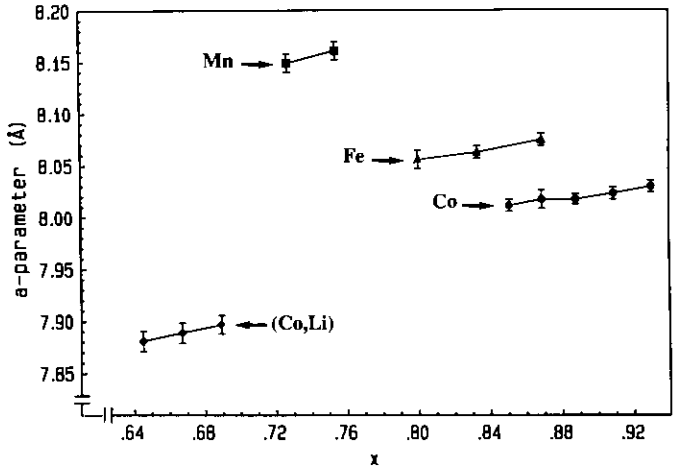

FIG. 2. Variation of the cubic unit-cell parameter of $Na_4Ba_xM_{4-x}F_{12}$ (M = Mn, Fe, Co) and $Na_{4-x}Li_xBa_xCo_{4-x}F_{12}$ with x.

As can be seen, those domains are smaller when the size of the transition ion becomes close to that of the sodium ion. Moreover, in the case of cobalt, which is the smallest ion of the series, the rate of sodium in the octahedral sites is the highest. Those results show that the stability of this type of phase cannot be deduced simply from the size of the ions occupying the octahedral sites. Moreover, it appears that with our experimental conditions, it is not possible to prepare the same phase in the case of Ni^{2+}. Another phase is stabilized which corresponds to the formula Na_2BaNiF_6 (*12*). The same phase has been isolated for cobalt also. It seems that the ionic radius of Co^{2+} represents the limit for the stabilization of this cubic phase. The variation of the unit cell parameter as a function of x is represented in Fig. 2. The a-parameter increases with x, as x represents the rate of sodium in the octahedral sites and the rate of barium in the icosahedral sites.

Structural Studies

The structures of $Na_4Ba_xCo_{4-x}F_{12}$ (x = 0.87) and $Na_{4-x}Li_xBa_xCo_{4-x}F_{12}$ (x = 0.67) have been refined from X-ray spectra using the Rietveld profile analysis. The crystallographic characteristics and the conditions of the diffraction experiments for the two phases are summarized in Table II. The coordinates of the atoms in $Na_4Ba_xFe_{4-x}F_{12}$ (x = 0.84) structure (*4*) (space group *Im*3) were adopted as the initial coordinates. The calculations considering a pseudo-Voigt lines profile, led to reliability factors R_I = 10.21% for $Na_4Ba_xCo_{4-x}F_{12}$ (x = 0.87) and R_I = 8.18% for $Na_{4-x}Li_xBa_xCo_{4-x}F_{12}$ (x = 0.67). The final values of the atomic and thermal parameters are listed in Table III. Table IV presents the interatomic distances. The observed and calculated spectra are presented in Figs. 3 and 4. As previously observed, the structure is closed related to the $[AC_3]B_4X_{12}$-ordered perovskite-like series (*4*). The 12*e* position is occupied only by the sodium atoms which are displaced off the planar environment of the C sites. The cobalt and the sodium atoms occupy simultaneously the B position (octahedral site), which is surprising, at first sight, because of the difference in their ionic radii ($r_{Co^{2+}}$ = 0.75 Å, r_{Na^+} = 1.02 Å) (*13*). However, the experimental B–F distance (2.070 Å) is in good agreement with the calculated one if one considers Co–F = 2.041 Å as in CoF_2 (*14*) and Na–F = 2.25 Å. For the phase $Na_{4-x}Li_xBa_xCo_{4-x}F_{12}$, the lithium and the

TABLE II

CRYSTALLOGRAPHIC DATA, RECORDING CONDITIONS, AND REFINEMENT RESULTS OF $Na_4Ba_xCo_{4-x}F_{12}$ (x = 0.87) AND $Na_{4-x}Li_xBa_xCo_{4-x}F_{12}$ (x = 0.67)

	$Na_4Ba_xCo_{4-x}F_{12}$ $x = 0.87$	$Na_{4-x}Li_xBa_xCo_{4-x}F_{12}$ $x = 0.67$
Symmetry	Cubic	Cubic
Space group	*Im*3	*Im*3
Unit-cell parameters	a = 8.0185(1)Å	a = 7.9006(1)Å
	V = 515.2(1)Å^3	V = 490.9(1)Å^3
	Z = 2	Z = 2
Angular range	10° < 2Θ < 120°	10° < 2Θ < 120°
Step count (2Θ)	0.02°	0.02°
Number of reflexions	32	29
Number of refined parameters	22	22
Profile function	Pseudo-Voight η = 0.5086	Pseudo-Voight η = 0.6148
	U = 0.334(2)	U = 0.021(1)
Profile parameters	V = 0.014(2)	V = 0.019(1)
	W = 0.0129(5)	W = 0.0124(5)
Shift of the origin (2Θ)	0.0823(3)	0.0422(3)
Reliability factors (%)	R_I = 10.21 Rp = 9.86	R_I = 8.18 Rp = 11.12
	Rwp = 13.11	Rwp = 14.43

cobalt are disordered in the octahedral site with a B–F distance of 2.040 Å. This value is also in good agreement with that calculated knowing that the ionic radii of these two cations are almost the same (r_{Li^+} = 0.76 Å) (*13*).

Magnetic Properties

Magnetic susceptibility. The thermal variation of the reciprocal susceptibilities of $Na_4Ba_xM_{4-x}F_{12}$ (M = Mn, Fe, Co) and $Na_{4-x}Li_xBa_xCo_{4-x}F_{12}$ evidenced an antiferromagnetic behavior with Neel temperatures ranging from 35 to 55 K. Figure 5 shows the case of $Na_4Ba_xCo_{4-x}F_{12}$ (x = 0.85). At $T > T_N$, this phase follows a Curie–Weiss law, the Curie constant being $C_{exp.}$ = 4.1, in good agreement with those generally observed for such cations. The variation of the maximum of susceptibility

TABLE III

ATOMIC POSITIONS AND ISOTROPIC THERMAL PARAMETERS B_{eq} (Å^2) IN $Na_4Ba_xCo_{4-x}F_{12}$ (x = 0.87) and $Na_{4-x}Li_xBa_xCo_{4-x}F_{12}$ (x = 0.67)

Atom	Site	x	y	z	B_{eq}(Å^2)
		$Na_4Ba_xCo_{4-x}F_{12}$ (x = 0.87)			
(0.5 Na)	12(e)	0.9502(9)	0	½	0.07
(0.131 Na + 0.869 Ba)	2(a)	0	0	0	0.73
(0.782 Co + 0.217 Na)	8(c)	¼	¼	¼	0.36
F	24(g)	0	0.3029(4)	0.2129(4)	0.80
		$Na_{4-x}Ba_xLi_xCo_{4-x}F_{12}$ (x = 0.67)			
(0.5 Na)	12(e)	0.9468(8)	0	½	0.5
(0.333 Na + 0.667 Ba)	2(a)	0	0	0	0.97
(0.833 Co + 0.167 Li)	8(c)	¼	¼	¼	0.27
F	24(g)	0	0.2987(4)	0.2076(4)	1.59

TABLE IV

MAIN INTERATOMIC DISTANCE (Å) AND ANGLES (°) IN $Na_4Ba_xCo_{4-x}F_{12}$ (x = 0.87) AND $Na_{4-x}Li_xBa_xCo_{4-x}F_{12}$ (x = 0.67)

$Na_4Ba_xCo_{4-x}F_{12}$ (x = 0.87)		$Na_{4-x}Li_xBa_xCo_{4-x}F_{12}$ (x = 0.67)	
Na–F	Ba(Na)–F	Na–F	Ba(Na)–F
4 × 2.360(3)	12 × 2.792(3)	4 × 2.323(4)	12 × 2.805(2)
2 × 2.652(3)	Co(Na)–F	2 × 2.540(4)	Co(Li)–F
F–F	6 × 2.070(3)	F–F	6 × 2.040(2)
4 × 2.971(3)	F–F	4 × 2.875(3)	F–F
3 × 3.414(3)	6 × 2.971(3)	3 × 3.280(3)	6 × 2.895(2)
2 × 3.161(3)	6 × 2.884(3)	2 × 3.180(3)	6 × 2.874(2)
F–Na–F	F–Co(Na)–F	F–Na–F	F–Co(Li)–F
4 × 72.44(10)	6 × 88.29(10)	4 × 72.30(10)	6 × 90.42(10)
2 × 92.64(10)	6 × 91.71(10)	2 × 89.83(10)	6 × 89.59(10)
2 × 84.06(10)	3 × 180	2 × 86.41(10)	3 × 180
1 × 80.14(10)		1 × 80.43(10)	
4 × 124.08(10)		4 × 125.46(10)	
2 × 160.52(10)		2 × 159.15(10)	

with different x representing the substitution rate of the transition element by Na is shown in Fig. 6 in the case of $Na_4Ba_xCo_{4-x}F_{12}$. In this system, T_N increases when x decreases. This phenomenon is logical if one considers that x characterizes the dilution rate of the magnetic system.

Magnetic structures. At T = 1.6 K, neutron diffraction patterns of $Na_4Ba_xMn_{4-x}F_{12}$ (x = 0.75) (Fig. 7b) and of

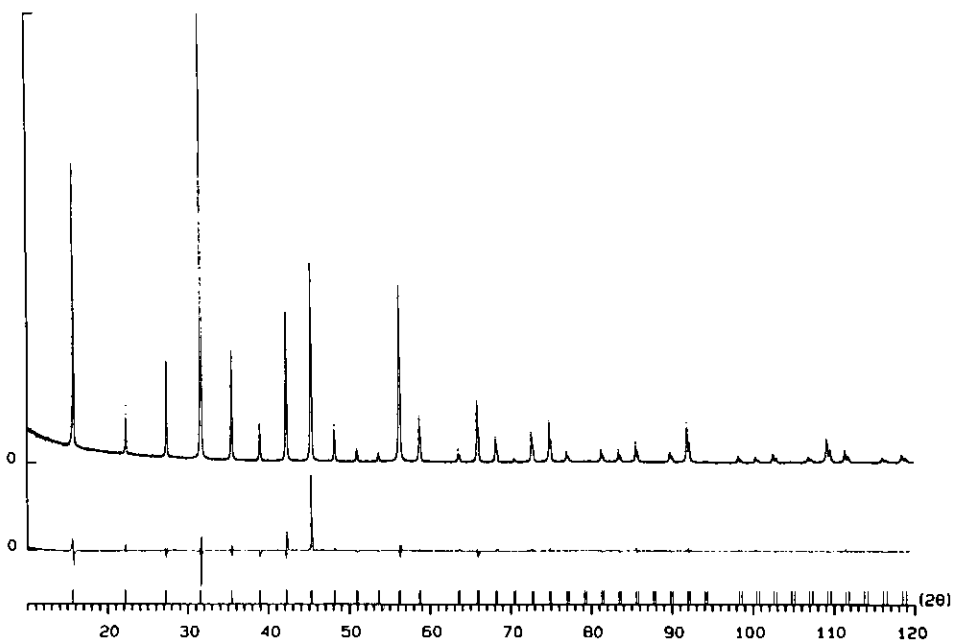

FIG. 3. The observed (···), calculated (top line), and difference (bottom line) XRD patterns of $Na_4Ba_xCo_{4-x}F_{12}$ (x = 0.87).

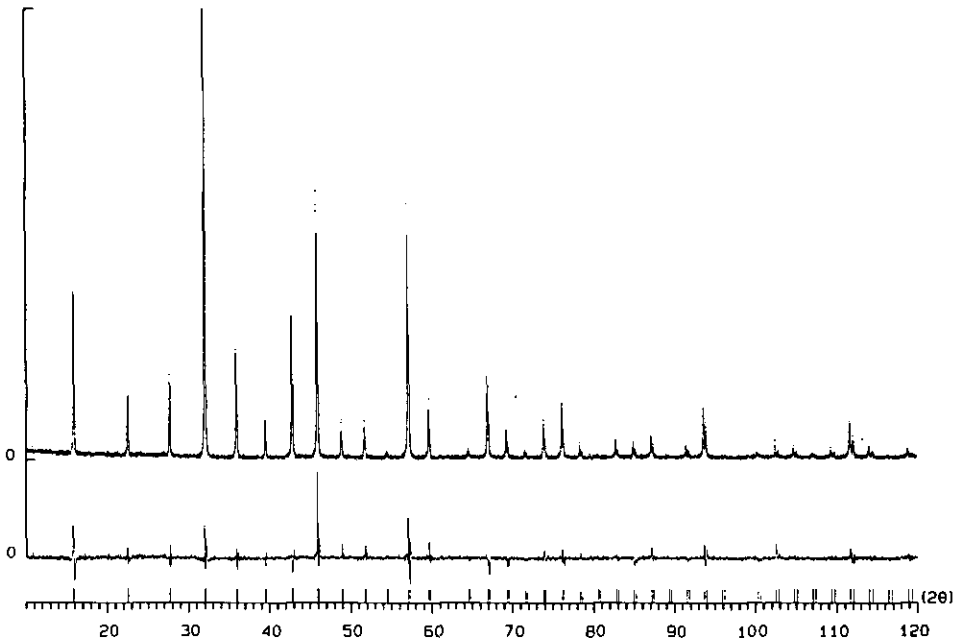

FIG. 4. The observed (···), calculated (top line), and difference (bottom line) XRD patterns of $Na_{4-x}Li_xBa_xCo_{4-x}F_{12}$ (x = 0.67).

$Na_4Ba_xFe_{4-x}F_{12}$ (x = 0.87) (Fig. 8b) exhibit magnetic reflexions which can be indexed in the crystallographic unit-cell (propagation vector **k**(0,0,0)). The thermal variations of the integrated intensities of the (111) and (311) magnetic Bragg peaks are shown in Fig. 9a for $Na_4Ba_xMn_{4-x}F_{12}$ (x = 0.75) and in Fig. 9b for $Na_4Ba_xFe_{4-x}F_{12}$ (x = 0.87), leading to Neel temperatures of 43 ± 1 K and 49 ± 1 K, respectively.

For $Na_4Ba_xMn_{4-x}F_{12}$ (x = 0.75), three

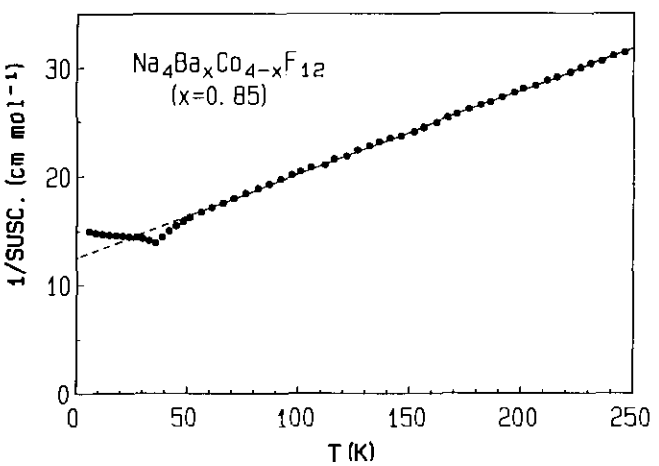

FIG. 5. Temperature dependence on the reciprocal molar magnetic susceptibility of $Na_4Ba_xCo_{4-x}F_{12}$ (x = 0.85).

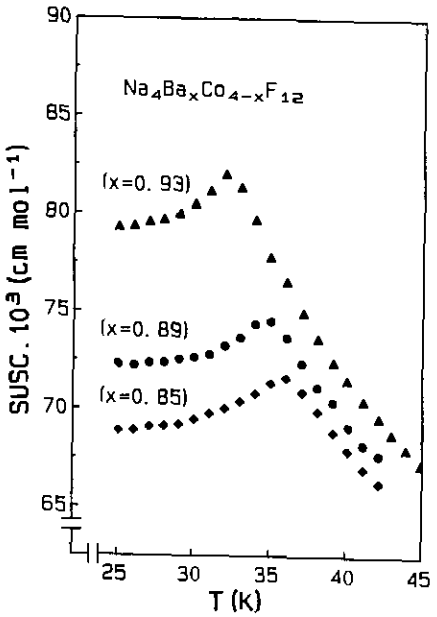

FIG. 6. Temperature dependence of the molar magnetic susceptibility of $Na_4Ba_xCo_{4-x}F_{12}$ for $x = 0.93$, 0.89, and 0.85.

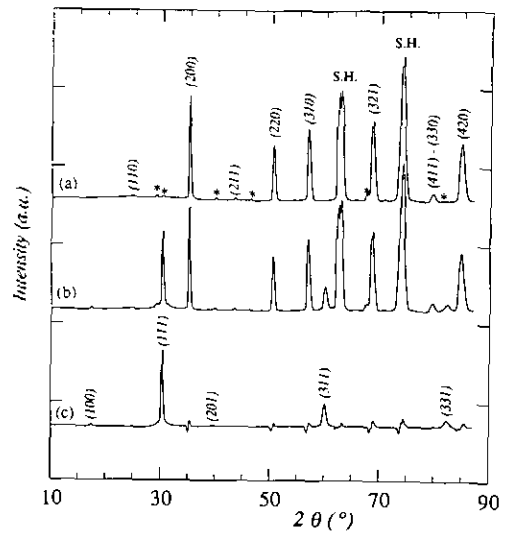

FIG. 8. Neutron diffraction patterns of Na_4Ba_x $Fe_{4-x}F_{12}$ ($x = 0.87$) at (a) $T = 60$ K, (b) $T = 1.6$ K, and (c) their difference. (*, impurity; S.H., sample holder).

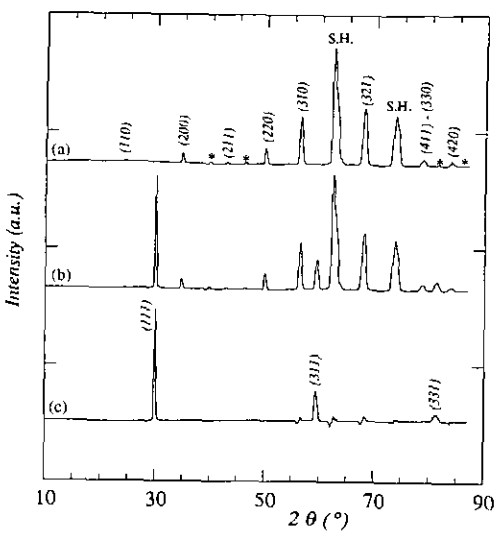

FIG. 7. Neutron diffraction patterns of Na_4 $Ba_xMn_{4-x}F_{12}$ ($x = 0.75$) at (a) $T = 60$ K, (b) $T = 1.6$ K, and (c) their difference (*, impurity; S.H., sample holder).

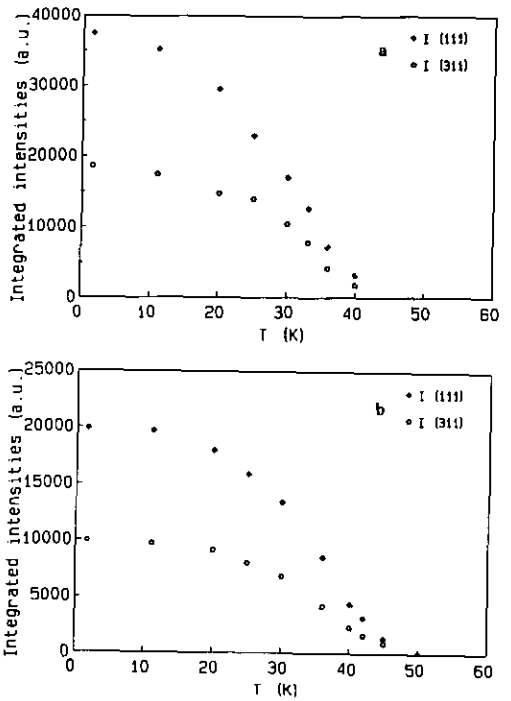

FIG. 9. Temperature dependence of the integrated intensities of the (◆) (111) and (○) (311) magnetic peaks of (a) $Na_4Ba_xMn_{4-x}F_{12}$ ($x = 0.75$) and (b) Na_4Ba_x $Fe_{4-x}F_{12}$ ($x = 0.87$).

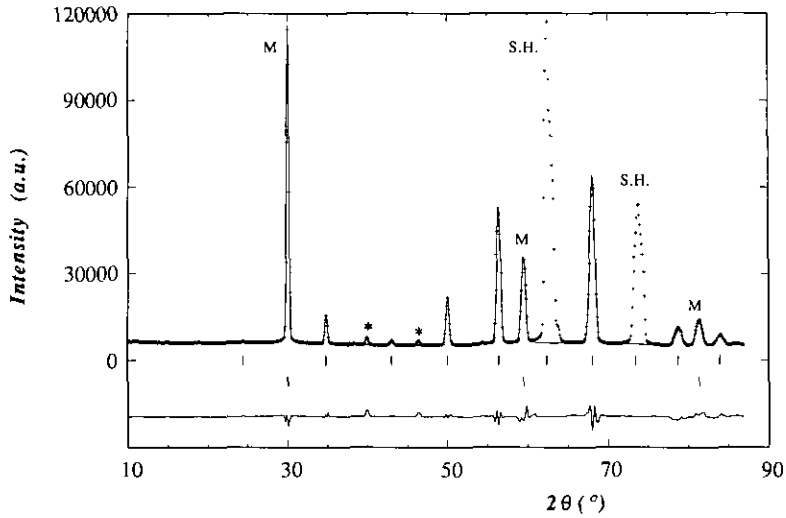

FIG. 10. The observed (+ + +), calculated (top line), and difference (bottom line) neutron diffraction patterns of $Na_4Ba_xMn_{4-x}F_{12}$ ($x = 0.75$) (*, impurity; S.H., sample holder).

magnetic peaks, (111), (311), (331), with an odd indices sum have been observed. Such a selection rule provides evidence for a strict antiparallelism between moments carried by atoms derived by lattice translation I. The refinement of nuclear and magnetic structures, considering an antiferromagnetic coupling of G-type, leads to the final magnetic and nuclear conventional R-factors 3.57% and 2.60%, respectively. The resulting magnetic moment of $4.92\mu_B$ for Mn^{2+} is in good agreement with the values commonly observed for this ion in octahedral sites. The observed and calculated spectra are given in Fig. 10.

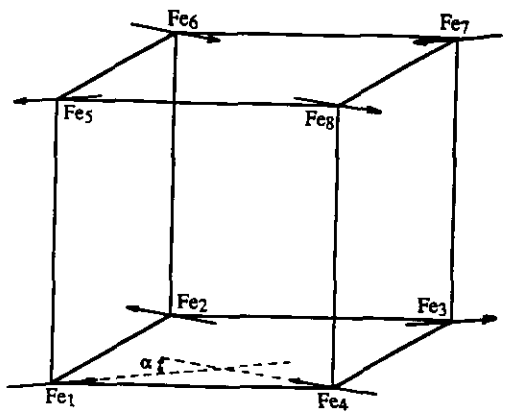

FIG. 11. The magnetic unit-cell of $Na_4Ba_xFe_{4-x}F_{12}$ ($x = 0.87$).

For $Na_4Ba_xFe_{4-x}F_{12}$ ($x = 0.87$), the most intense peaks are the same as in the manganese phase, indicating a 3D antiferromagnetic coupling. However, the existence of the weak magnetic peaks (100) and (201) (Fig. 8) which do not satisfy the condition of odd h,k,l indices can be explained by a small deviation from the preceeding model. The best result is actually obtained for the canted structure illustrated in Fig. 11. The absence of spontaneous magnetization for $T < T_N$ indicates that the resultant moment in the magnetic unit-cell is equal to zero, leading to a hidden canting. For such a canted structure, the spin reversal is different from the 180° between two magnetic atoms in positions x,y,z and x',y',z', with $x' = x + \frac{1}{2}$, $y' = y$, $z' = z$, and $x' = x$, $y' = y + \frac{1}{2}$, $z' = z$. The refinements of the nuclear and magnetic structures converge to the conventional R-factors of 2.26% and 5.57%, respectively. The final value for the canting angle is 15°. The magnetic moment for the Fe^{2+} ion ($3.93\mu_B$) is in good agreement with the values expected for this ion in octahedral sites ($\mu_{Fe^{2+}} \approx 4\mu_B$). The

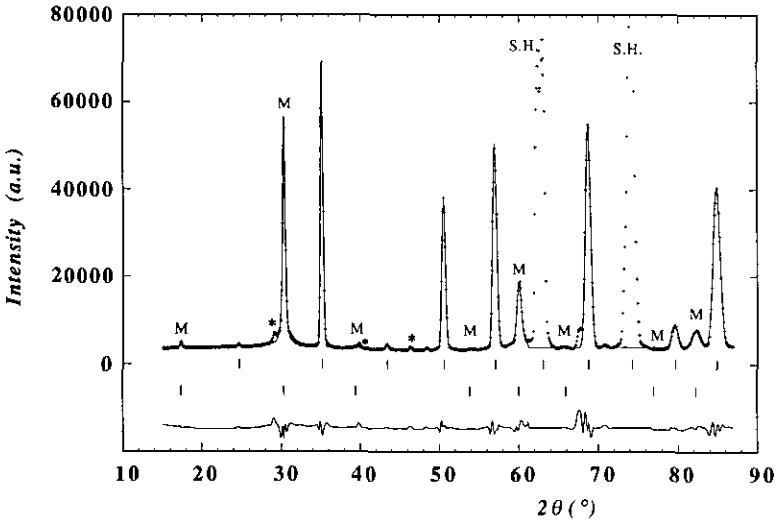

FIG. 12. The observed (+ + +), calculated (top line), and difference (bottom line) neutron diffraction patterns of $Na_4Ba_xFe_{4-x}F_{12}$ ($x = 0.87$) (*, impurity; S.H., sample holder).

observed and calculated spectra are given in Fig. 12.

Conclusion

The study of the ternary systems $NaF–BaF_2–MF_2$ (M = Mn, Fe, Co) shows the existence of a new cubic perovskite-type structure (i.e., $Im3$) with a unit cell constant which is twice that of a simple ABX_3 perovskite. The doubling of the unit cell is due to the partial collapse of the BX_3 framework. This collapse is achieved by a tilting of the BX_6 octahedra around one of their three axes as in the oxide series $[AC_3]B_4O_{12}$. Two distinct sites A and C are therefore generated. The C sites (CN = 4) are occupied by Jahn-Teller cations in the oxide series, but in the fluoride series the sodium atoms are displaced off this position in a triangular prism which is more suitable for this cation. The exact cationic distribution has been determined by X-ray and neutron diffraction. The cationic disordering in the different sites is at the origin of the homogeneity range of this phase. The size of the cobalt(II) represents the lower limit for $3d$ transition elements which can be stabilized in this type of structure. Only in the case of the phase with cobalt has the substitution of Na atoms in the octahedral sites by Li been possible. All these phases exhibit antiferromagnetic behavior. The magnetic structure of $Na_4Ba_xMn_{4-x}F_{12}$ ($x = 0.75$) consists in an antiferromagnetic ordering of G-type whereas for $Na_4Ba_xFe_{4-x}F_{12}$ ($x = 0.87$) a small canting of the magnetic moments has been observed.

References

1. A. DE KOZAK, M. SAMOUËL, J. RENAUDIN, AND G. FEREY, *Eur. J. Solid State Inorg. Chem.* **25,** 15 (1988).
2. A. DE KOZAK, M. SAMOUËL, J. RENAUDIN, AND G. FEREY, *Eur. J. Solid State Inorg. Chem.* **27,** 771 (1990).
3. G. FRENZEN, S. KUMMER, W. MASSA, AND D. BABEL, *Z. Anorg. Allgem. Chem.* **553,** 75 (1987).
4. J. DARRIET, M. DUCAU AND A. TRESSAUD, *Eur. J. Solid State Inorg. Chem.* **29,** 395 (1992).
5. A. DESCHANVRES, B. RAVEAU, AND F. TOLLEMER, *Bull. Soc. Chim. Fr.* 4077 (1967).
6. V. PROPACH AND D. REINEN, *Inorg. Nucl. Chem. Lett.* **7,** 569 (1971).
7. M. MAREZIO, P. D. DERNIER, J. CHENEVAS, AND J. C. JOUBERT, *J. Solid State Chem.* **6,** 16 (1973).

8. V. PROPACH, *Z. Anorg. Allgem. Chem.* **435,** 161 (1977).
9. H. M. RIETVELD, *Acta Crystallogr.* **22,** 151 (1967).
10. J. RODRIGUEZ-CARJAVAL, *in* "Abstracts of the Satellite Meeting on Powder Diffraction of the XV Congress of the IUCr," Toulouse, France, 1990, p. 127.
11. E. J. LISHER AND J. B. FORSYTH, *Acta Crystallogr. Sect. A* **27,** 545 (1971).
12. J. DARRIET, unpublished work.
13. R. D. SHANNON, *Acta Crystallogr. Sect. A* **32,** 751 (1976).
14. W. H. BAUR, *Naturwissenschaften* **12,** 349 (1957).